Effective elastic thickness and heat flux estimates on Ganymede

Francis Nimmo
Department of Geological Sciences, University College London, UK

Robert T. Pappalardo
Laboratory for Atmospheric and Space Physics, University of Colorado, Boulder, Colorado, USA

Bernd Giese
DLR, Berlin, Germany

Received 23 August 2001; revised 6 November 2001; accepted 14 November 2001; published 13 April 2002.

[1] We identify sites of apparent flexural uplift at rift zone boundaries on Ganymede using Galileo stereo-derived topography. The estimated effective elastic thickness t_e is 0.9–1.7 km for a nominal Young's modulus of 1 GPa. Using a viscoelastic model of the ice crust we find that the temperature defining the base of the elastic layer is <185 K for likely strain rates. The inferred local heat flux during deformation is less than 245 mW m^{-2}, and probably close to 100 mW m^{-2}. The stresses required to cause fault motion are around 1 MPa. Both the high heat flux and the high stresses are consistent with estimates of these quantities during an episode of transient tidal heating in Ganymede's past. *INDEX TERMS:* 6218 Planetology: Solar System Objects: Jovian satellites; 5418 Planetology: Solid Surface Planets: Heat flow; 8149 Evolution of the Earth: Planetary tectonics (5475); 8164 Evolution of the Earth: Stresses—crust and lithosphere

1. Introduction

[2] The icy Galilean satellite Ganymede was apparently heavily tectonized during its history [*Shoemaker et al.*, 1982]. The absolute age at the end of this deformation event is uncertain [*Zahnle et al.*, 1998]. One of the results of the tectonism is small-scale ridges, interpreted as tilted fault blocks caused by extension [*Pappalardo et al.*, 1998].

[3] Both silicate and icy planetary bodies tend to possess a rigid outer layer that can support loads such as mountain chains and rift valleys. The rigidity of this layer is often expressed as an effective elastic thickness, t_e. The depth to the base of the elastic layer is commonly represented by a particular isotherm [*Watts and Daly*, 1981]. Thus, if t_e can be estimated, it is possible to infer the near-surface heat flux, which is a key parameter to understanding the interiors of planetary bodies.

[4] Topography may be used to estimate t_e by fitting an elastic model to profiles that are assumed to be flexural. For instance, *Brown and Phillips* [1999] estimated t_e from rift flank uplift at the Rio Grande Rift, and *Barnett et al.* [2002] used a similar technique for rift flanks on Venus.

[5] In this paper, we identify topographic features of apparent flexural origin on Ganymede, and use them to obtain estimates of t_e. We then discuss the implications of these results for the thickness of the conductive layer, the heat flux and the likely stresses at the time of deformation.

0094-8276/02/2001GL013976$05.00

2. Observations

[6] We investigate regions of Ganymede imaged at high resolution and in stereo during Galileo orbit G28 (Figure 1) [*Head et al.*, 2001]. Stereographic methods have been used to reconstruct the topography of the areas [*Giese et al.*, 1998, 2001], allowing extraction of detailed topographic profiles. Figure 2 shows the mean topographic profiles from the transects in Figure 1, with bounds of ± one standard deviation calculated from the profiles. The consistency and shape of the rift flank rises suggest a flexural origin.

[7] Images of a boundary between dark and bright terrain (Figure 1a) reveal the extensional tectonic nature of the transition, while the relatively smooth nature of the bright terrain is suggestive of icy volcanism there [*Head et al.*, 2001]. The deep bounding trough may owe its origin to hanging wall rollover above a deeply penetrating normal fault, as hypothesized elsewhere on Ganymede [*Pappalardo et al.*, 1998]. Flexural uplift within the bright terrain eastward of the bounding trough is inferred from the stereo-derived topographic data (Figure 2, profile p1).

[8] Images targeted to Arbela Sulcus, a bright northeast-trending groove lane, reveal pervasive east-west oriented tectonism within dark terrain that flanks it (Figure 1b). This area of rifted dark terrain appears to be an example of tectonic resurfacing [*Head et al.*, 1997], in which tectonism has destroyed preexisting terrain in the absence of icy volcanism. Prominent fault-induced topography and the apparent signature of flexure is revealed by the stereo image data along the margin between relatively undeformed terrain to the south and pervasively faulted terrain to the north (Figure 2, profile p2).

3. Theory and Method

3.1. Flexure

[9] The wavelength of deformation induced by a load on an elastic plate is governed by the flexural parameter α, which is given by

$$\alpha = \left(\frac{E\,t_e^3}{3(1-\nu^2)\Delta\rho\,g}\right)^{1/4} \tag{1}$$

where E is the Young's Modulus, ν is the Poisson's ratio of the material, g is the gravitational acceleration and $\Delta\rho$ is the density contrast between the crust and the material above it [*Turcotte and Schubert*, 1982].

[10] In this study, we follow the method of *Barnett et al.* [2002] in which we calculate the misfit between the topographic observations and a model flexural profile of a broken plate (appropriate

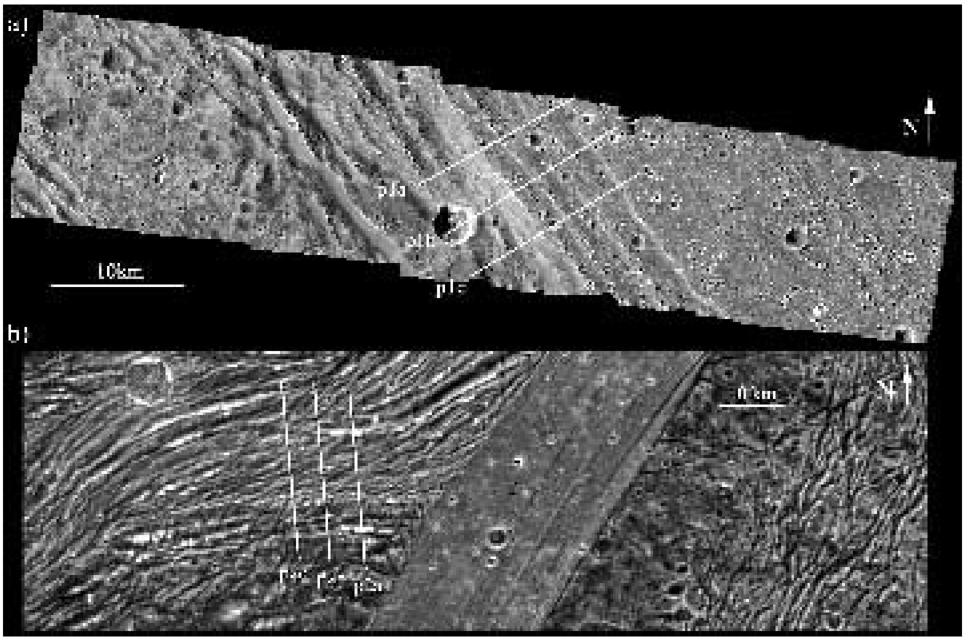

Figure 1. (a) Image mosaic of Galileo G28 images (20 m/pixel) taken at the boundary of Nicholson Regio (left) with Harpagia Sulcus (right). Parallel topographic profiles are averaged to produce the curves shown in Figure 2. Stereo data have horizontal resolution of 600 m, and vertical resolution of 15–30 m. (b) Galileo G28 image mosaic (130m/pixel) in Nicholson Regio/Arbela Sulcus. Stereo data have horizontal resolution of 600 m, and vertical resolution of 15–25 m.

if the rift-zone bounding fault has penetrated the elastic layer). We vary α, the position of the break (i.e. the point of maximum flexure), and two geometric parameters controlling the amplitude of the deflection to minimize the misfit. We then use equation (1) to determine the best-fit elastic thickness.

3.2. Maxwell Time

[11] Geological materials tend to behave elastically on timescales short relative to a reference time known as the Maxwell time

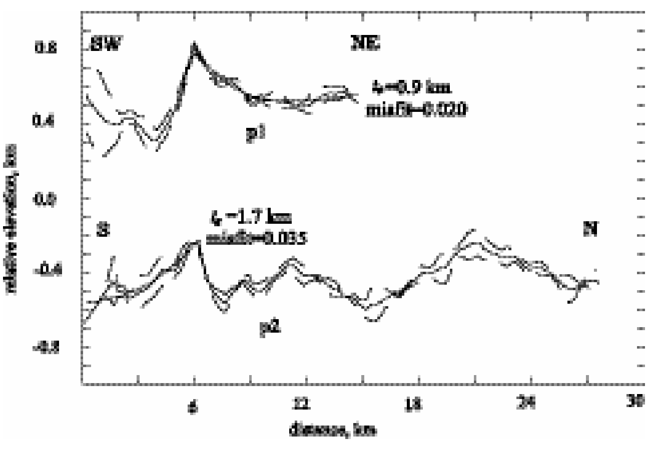

Figure 2. Stereo-derived mean topographic profiles and best-fit flexural models. The mean was calculated after aligning the three profiles on the point of steepest gradient. Only points using all three profiles are plotted. Solid line is the mean profile; dashed lines are ± one standard deviation calculated from the three profiles; dotted line is the best-fit flexural profile. The Young's modulus is 1 GPa.

(τ_M) and in a viscous fashion on longer timescales. The Maxwell time is given by [*Ranalli*, 1995]

$$\tau_M = \eta_e/\mu \tag{2}$$

where μ is the rigidity modulus (= $E/2(1+\nu)$) and η_e is the effective viscosity. For a specified strain rate $\dot{\epsilon}$ the effective viscosity in the dislocation creep regime is given by [*Durham et al.*, 1997]:

$$\eta_e = \frac{1}{3} A^{-\frac{1}{n}} d^{p/n} \dot{\epsilon}^{\frac{1}{n}-1} \exp(Q/nRT) \tag{3}$$

where T is temperature, R is the gas constant, d is grain size and A, Q, p and n are rheological constants. Material close to the surface will be cold and thus behave in an elastic fashion; deeper material will behave in a viscous fashion. The crossover depth occurs at the point where the product of the material's Maxwell time and the strain rate, known as the Deborah number $De \sim 0.01$ [*Mancktelow*, 1999]. This depth will define the base of the elastic layer; we assume that the elastic layer extends to the surface.

[12] A simple solution may be obtained for the temperature T_M at the base of the elastic layer. Combining equations (2) and (3) we obtain

$$T_M = \frac{Q}{nR}\left[\ln\left(\frac{3DeA^{\frac{1}{n}}\mu}{d^{p/n}\dot{\epsilon}^{\frac{1}{n}}}\right)\right]^{-1}. \tag{4}$$

[13] At sufficiently low strain rates equation (4) predicts that viscous flow will extend to the surface; in reality, brittle failure (which we do not model) may become important at shallow depths.

[14] The conductivity of ice k varies as $567/T$ [*Klinger*, 1980]. Assuming a conductive lid in which no heat generation occurs, with top and bottom temperatures T_s and T_b, respectively, the heat flux F is given by:

$$\frac{F}{567} = \frac{\ln(T_M/T_s)}{t_e}. \tag{5}$$

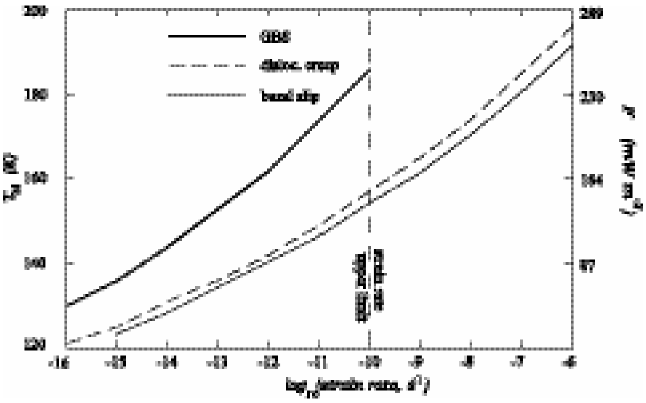

Figure 3. Temperature defining the base of the elastic layer (T_M - equation (4)) as a function of strain rate for three different rheologies of *Goldsby and Kohlstedt* [2001]. Heat flux (right-hand scale) is calculated using equation (5) and assuming t_e = 1 km.

[15] Although equations (4) and (5) do not represent the full complexity of likely ice behaviour, and the heat flux estimates thus derived are somewhat uncertain, more complicated methods are unlikely to reduce the uncertainty until the parameters relevant to Ganymede are better known.

3.3. Parameters

[16] The Young's modulus of ice on Europa was assumed to lie between 6×10^7 and 6×10^9 Pa by [*Williams and Greeley*, 1998] and has been measured at 9 GPa [*Gammon et al.*, 1983]. We use a nominal value of 1 GPa for Ganymede based on terrestrial modelling results [*Vaughan*, 1995]. We also assume a Poisson's ratio of 0.33, a density of 1000 kg m^{-3} and a gravity of 1.4 m s^{-2}. The temperature at the surface is assumed to be 120 K. The mean thermal conductivity over the range 120–200 K is 3.6 W m^{-1} K^{-1}.

[17] The dominant deformation mechanisms of ice are likely to be stress-dependent [*Goldsby and Kohlstedt*, 2001] at likely near-surface conditions on Ganymede. Given the uncertainties, we use three rheologies from *Goldsby and Kohlstedt* [2001]: dislocation creep, grain boundary sliding (GBS) accommodated basal slip (both at T < 258 K), and basal slip-accommodated GBS. For the grain-size dependent cases we assume a grain size of 1 mm.

[18] Strain rates during deformation of Ganymede are not well constrained. *Collins et al.* [1998] and *Dombard and McKinnon* [2002] determined strain rates of $\sim 10^{-16}$–10^{-14} s^{-1} for specific areas of grooved terrain. Strain rates are unlikely to ever have exceeded the current, tidally-induced values on Europa of $\sim 10^{-10}$ s^{-1} [*Ojakangas and Stevenson*, 1989].

4. Results

[19] Figure 2 shows the mean topography and the minimum misfit model topographic profiles. It demonstrates that a t_e of 0.9–1.7 km fits the data for a Young's modulus of 10^9 Pa. The lower bound on t_e is tightly constrained, whereas the upper bound is less certain. Both profiles fit a t_e of 1.0 km with a misfit within 5% of the minimum misfit value. Because the profiles constrain α there is a tradeoff between E and t_e (equation 1). For the upper and lower bounds of 6×10^7 Pa and 9×10^9 Pa we found values for t_e of 2.5 km and 0.5 km, respectively, for the profile p1.

[20] Figure 3 shows how the temperature defining the base of the elastic layer, T_M (equations 4 and 5) varies with strain rate $\dot{\epsilon}$ for the three ice rheologies assumed. For likely strain rates ($\dot{\epsilon} < 10^{-10}$ s^{-1}) T_M is generally less than 185 K. The corresponding homologous temperature (i.e. T_M normalized to the melting temperature) is 0.45–0.69, which overlaps the range of 0.6 ± 0.05 found for terrestrial oceanic lithosphere [*Watts and Daly*, 1981].

[21] Given T_M and t_e we can calculate F using equation (5). The resulting values of F for a t_e of 1 km are shown in Figure 3 and demonstrate that $F \leq 245$ mW m^{-2}. A reduction in surface temperature of 20 K would increase the heat flux by a factor of 1.5–2 for T_M = 140–180K.

[22] For GBS at strain rates of $\sim 10^{-14}$ s^{-1} [*Dombard and McKinnon*, 2002] the implied heat flux is 100 mW m^{-2}. *Dombard and McKinnon* [2002] found values of 30–300 mW m^{-2} for grooved terrain, assuming an average thermal conductivity of 3 W m^{-1} K^{-1}.

5. Discussion and Conclusions

[23] The flexural profiles in Figure 1 give a reasonably well constrained effective elastic thickness of about 1 km. On Earth, effective elastic thicknesses are usually correlated with, and a little smaller than, the depth to the base of the brittle layer [*McKenzie and Fairhead*, 1997]. *Dombard and McKinnon* [2002] estimated that the brittle-ductile transition occurred at $\sim$1–2 km at the time of grooved terrain formation on Ganymede, which is consistent with our results. For Europa, *Williams and Greeley* [1998] and *Tufts et al.* [1997] found t_e values of 0.15–1.0 km and $\sim$0.4 km, respectively, by looking at apparent flexure of features.

[24] The mechanical properties derived above represent the state of the lithosphere at the end of local deformation, and presumably are not indicative of present-day properties. Furthermore, the extension will cause the heat flux to be higher, and t_e lower, than in surrounding less deformed regions. In addition, the heavily fractured near-surface layer may not behave in an elastic fashion, so that the depth to T_M may be an underestimate, and the heat flux an overestimate.

[25] Given the fault block topography and a value of t_e, it is possible to estimate the stresses arising on the rift-bounding faults [*Foster and Nimmo*, 1996]. We assume a typical fault throw of 0.4 km, a t_e of 1 km and a rift width of 5–10 km and obtain maximum resolved shear stresses (*i.e.* fault strengths) of 0.2–1.0 MPa. Such stresses are at least an order of magnitude greater than present-day diurnal tidal stresses on Europa [*Hoppa et al.*, 1999]. However, tidal stresses scale with orbital eccentricity, so the stresses could have approached the magnitude necessary for fault motion during a hypothesized episode of tidal heating earlier in Ganymede's history [*Showman and Malhotra*, 1997]. Alternatively, nonsynchronous rotation [*Leith and McKinnon*, 1996] or vigorous convection [*McKinnon*, 1999] might have produced stresses of a few MPa.

[26] The inferred local heat flux of $\sim$100 mW m^{-2} depends on relating the thermal structure of the lithosphere to t_e, and is correspondingly less certain. Moreover, the heat flux inferred only applies to the deforming area, and may be several times the background heat flux. Nonetheless, it is an order of magnitude greater than the likely present-day radiogenic heat flux. Assuming that Jupiter's tidal dissipation factor Q_J is close to its minimum value of 3×10^4, the heat flux during a tidal resonance episode could have been of order 100 mW m^{-2} [*Showman and Malhotra*, 1997], sufficient to account for the heat flux inferred here.

[27] **Acknowledgments.** FN thanks the California Institute of Technology, Magdalene College, Cambridge, and the Royal Society for their financial support. We also acknowledge the help of two anonymous reviewers.

References

Barnett, D. N., F. Nimmo, and D. McKenzie, Flexure of Venusian lithosphere measured from residual topography and gravity, *J. Geophys. Res.*, in press, 2002.

Brown, C. D., and R. J. Phillips, Flexural rift flank uplift at the Rio Grande rift, New Mexico, *Tectonics*, *18*, 1275–1291, 1999.

Collins, G. C., J. W. Head, and R. T. Pappalardo, The role of extensional instability in creating Ganymede grooved terrain: Insights from Galileo high-resolution stereo imaging, *Geophys. Res. Lett.*, *25*, 233–236, 1998.

Dombard, A. J., and W. B. McKinnon, Formation of grooved terrain on Ganymede, *Icarus*, 2002.

Durham, W. B., S. H. Kirby, and L. A. Stern, Creep of water ices at planetary conditions: A compilation, *J. Geophys. Res.*, *102*, 16,293–16,302, 1997.

Foster, A., and F. Nimmo, Comparisons between the rift systems of East Africa, Earth, and Beta Regio, Venus, *Earth Planet. Sci. Lett.*, *143*, 183–195, 1996.

Gammon, P. H., H. Kiefte, and M. J. Clouter, Elastic constants of ice from samples by Brillouin spectroscopy, *J. Phys. Chem.*, *87*, 4025–4029, 1983.

Giese, B., J. Oberst, T. Roatsch, G. Neukum, J. W. Head, and R. T. Pappalardo, The local topography of Uruk Sulcus and Galileo Regio obtained from stereo images, *Icarus*, *135*, 303–316, 1998.

Giese, B., R. Wagner, G. Neukum, R. Pappalardo, J. W. Head, and the Galileo Imaging Team, The topography of Ganymede's Arbela Sulcus, Lunar Planet. Sci. Conf., XXXII, abstract 1743, Lunar and Planetary Institute, Houston (CD-ROM), 2001.

Goldsby, D. L., and D. L. Kohlstedt, Superplastic deformation of ice: Experimental observations, *J. Geophys. Res.*, *106*, 11,017–11,030, 2001.

Head, J. W., R. Pappalardo, G. Collins, and R. Greeley, Tectonic resurfacing on Ganymede and its role in the formation of grooved terrain (abstract), Lunar Planet. Sci. Conf., XXVIII, 535–536, 1997.

Head, J. W., R. Pappalardo, G. Collins, N. Spaun, B. Nixon, R. Wagner, B. Giese, G. Neukum, and the Galileo SSI Team, Ganymede: Very high resolution data from G28 reveal new perspectives on processes and history, Lunar Planet. Sci. Conf., XXXII, abstract 1980, Lunar and Planetary Institute, Houston (CD-ROM), 2001.

Hoppa, G. V., B. R. Tufts, R. Greenberg, and P. E. Geissler, Formation of Cycloidal Features on Europa, *Science*, *285*, 1899–1902, 1999.

Klinger, J., Influence of a phase transition of ice on the heat and mass balance of comets, *Science*, *209*, 271–272, 1980.

Leith, A. C., and W. B. McKinnon, Is there evidence for polar wander on Europa?, *Icarus*, *120*, 387–398, 1996.

Mancktelow, N. S., Finite-element modelling of single-layer folding in elasto-viscous materials: The effect of initial perturbation geometry, *J. Struct. Geol.*, *21*, 161–177, 1999.

McKenzie, D., and D. Fairhead, Estimates of the effective elastic thickness of the continental lithosphere from Bouguer and free air gravity anomalies, *J. Geophys. Res.*, *102*, 27,523–27,552, 1997.

McKinnon, W. B., Convective instability in Europa's floating ice shell, *Geophys. Res. Lett.*, *26*, 951–954, 1999.

Ojakangas, G. W., and D. J. Stevenson, Thermal state of an ice shell on Europa, *Icarus*, *81*, 220–241, 1989.

Pappalardo, R. T., J. W. Head, G. C. Collins, R. L. Kirk, G. Neukum, J. Oberst, B. Giese, R. Greeley, C. R. Chapman, P. Helfenstein, J. M. Moore, A. McEwen, B. R. Tufts, D. A. Senske, H. H. Breneman, and K. Klaasen, Grooved terrain on Ganymede: First results from Galileo high-resolution imaging, *Icarus*, *135*, 276–302, 1998.

Ranalli, G., *Rheology of the Earth*, 413 pp., Chapman & Hall, New York, 1995.

Shoemaker, E. M., B. K. Lucchitta, J. B. Plescia, S. W. Squyres, and D. E. Wilhelms, The geology of Ganymede, in *Satellites of Jupiter*, edited by D. Morrison, pp. 435–520, Univ. of Ariz. Press, Tucson, 1982.

Showman, A. P., and R. Malhotra, Tidal evolution into the Laplace resonance and the resurfacing of Ganymede, *Icarus*, *127*, 93–111, 1997.

Tufts, B. R., R. Greenberg, P. Geissler, G. Hoppa, R. Pappalardo, and R. Sullivan, Crustal displacement features on Europa, *Geol. Soc. Am. Abstr. Programs*, *29*(A-312), 1997.

Turcotte, D. L., and G. Schubert, *Geodynamics*, 450 pp., John Wiley, New York, 1982.

Vaughan, D. G., Tidal flexure at ice shell margins, *J. Geophys. Res.*, *100*, 6213–6224, 1995.

Watts, A. B., and S. F. Daly, Long wavelength gravity and topography anomalies, *Ann. Rev. Earth Planet. Sci.*, *9*, 415–458, 1981.

Williams, K. K., and R. Greeley, Estimates of ice thickness in the Conamara Chaos region of Europa, *Geophys. Res. Lett.*, *25*, 4273–4276, 1998.

Zahnle, K., L. Dones, and H. F. Levison, Cratering rates on the Galilean satellites, *Icarus*, *136*, 202–222, 1998.

F. Nimmo, Department of Geological Sciences, University College London, London WC1E 6BT, UK. (nimmo@gps.caltech.edu)

R. T. Pappalardo, Laboratory for Atmospheric and Space Physics, Campus Box 392, University of Colorado, Boulder CO 80309, USA. (robert. pappalardo@colorado.edu)

B. Giese, DLR, Rutherfordstrasse 2, 12489 Berlin, Germany. (bernd. giese@dlr.de)